IEEE Photonics Journal
An IEEE Photonics Society Publication

Open Access

Tapered Optical Fiber Couplers Fabricated by Droplet-Based Chemical Etching

Volume 9, Number 5, October 2017

Gyeongho Son
Youngho Jung
Kyoungsik Yu

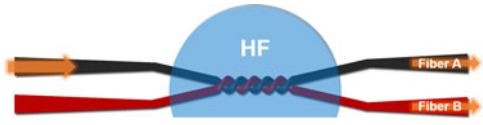

DOI: 10.1109/JPHOT.2017.2738661
1943-0655

IEEE photonics SOCIETY

IEEE

Tapered Optical Fiber Couplers Fabricated by Droplet-Based Chemical Etching

Gyeongho Son, Youngho Jung, and Kyoungsik Yu

School of Electrical Engineering, Korea Advanced Institute of Science and Technology, Daejeon 34141, South Korea

DOI:10.1109/JPHOT.2017.2738661

Manuscript received June 23, 2017; revised July 26, 2017; accepted August 7, 2017. Date of publication August 11, 2017; date of current version September 1, 2017. This work was supported in part by the research fund of Signal Intelligence Research Center supervised by the Defense Acquisition Program Administration and the Agency for Defense Development of Korea. Corresponding author: Kyoungsik Yu (e-mail: ksyu@kaist.edu).

Abstract: This paper presents a fabrication method for 2 × 2 twisted fiber-optic directional couplers based on biconical low-loss tapered optical fibers using a two-step wet-etching technique with hydrofluoric acid-based droplets and surface tension-driven flows. The droplet-based wet etching of optical fibers allows us simple and cost-effective fabrication of tapered fibers and multiports directional couplers. The simulation results agree well with the experimental observations on the propagation losses, which can be monitored in real-time by measuring the transmitted optical powers during the chemical etching process. The fabricated 2 × 2 fiber-optic directional coupler shows wavelength-insensitive operation within the telecommunication C-band with an excess insertion loss of less than 0.5 dB.

Index Terms: Fiber optics systems, waveguides, waveguide devices.

1. Introduction

Optical directional couplers are of considerable interest in view of their versatile applications in fiber-optic communication systems [1]–[4] and sensor systems [5]–[8]. The fiber-optic couplers have been considered as one of the most fundamental optical components in the optical fiber-based devices and systems due to their basic functionality, which is the combination and division of optical signals. For example, in the optical communication systems, they can be used in a number of applications, such as power combiner/dividers [1], add-drop wavelength division multiplexers [2], modulators [3], and switches [4].

Fiber-to-fiber optical coupling is usually achieved through evanescent wave coupling, which requires sufficient exposure and close proximity of the fiber cores for intimate interaction of the evanescent mode profiles that extend outside the waveguide core regions. For typical standard single-mode optical fibers (SMFs), however, the guided optical modes cannot closely interact with the external electromagnetic fields outside the fiber structure because the fiber core region is surrounded by the cladding layer, leaving only a very small fraction of the optical mode profiles outside the fiber cladding. Thus, the optical fibers with wavelength- or subwavelength-scale core/cladding dimensions are necessary to spread the evanescent components of the mode profile outside the fiber and couple the optical energy to the other waveguides. To efficiently transfer the guided optical energy to the evanescent field region, however, we must avoid abrupt and rapid variation of the fiber core/cladding diameter profiles, which might result unfavorable impacts, such as back-reflection and

scattering, on the propagating light [9], [10]. To address such issues, tapered optical fibers (TOFs) with adiabatically tapered core transition have been proposed and experimentally demonstrated [11]–[17].

There are three general techniques to fabricate TOF-based fiber-optic directional couplers starting from the conventional optical fibers. Heating-and-pulling of twisted multiple strands of optical fibers is the most common way to fabricate the fiber-optic couplers [11], [18], [19]. The couplers made by the heating-and-pulling method show very low optical losses and also provide broad operation wavelength ranges [11]. The couplers can also be made by twisting the pulled single-strand fibers [5], [8]. The heat-based fabrication methods, however, usually require precise mechanical control of fiber pulling stages as well as high-power heat sources, such as flames [14], micro-ceramic heaters [15], and CO_2 lasers [20], to melt the glass materials. This method also produces unnecessarily long taper regions [15]. The second fabrication method is the mechanical polishing, and has also been extensively investigated to demonstrate efficient coupling between the optical fibers and/or waveguides [21], [22]. Unfortunately, this method also requires precise and repeatable control of the polished fiber cores and precision alignment between them. The physical polishing of the optical fibers into the D-shaped core cross-section typically results in asymmetric optical mode profiles and induces birefringence [23], [24].

The TOFs, which are the essential components for the fiber-optic coupler configurations, can also be obtained by chemically etching the optical fibers until most of the cladding region is removed, for example, by hydrofluoric (HF) acid-based etchant solutions [1], [10], [25]. Although the power coupling ratio can be monitored in real-time during the etching process as demonstrated in [1], this chemical etching-based fabrication method is known to show a relatively non-uniform and uncontrolled etch rate when the whole fiber tip is dipped into the bulk HF-based solutions, and such non-uniformity may induce severe optical scattering losses because of abrupt tapering profiles and random roughness on the etched surface [10], [25]. To minimize such scattering problems and to obtain the smooth conical taper region, a micro-droplet-based HF acid etching method, taking advantages of surface tension-driven flows of liquid etchant (Marangoni effects [26]), was introduced [16]. This approach results in adiabatically decreasing and smooth fiber diameter profiles toward the fiber waist region without abrupt corrugations over sufficiently long distances on the order of one millimeter, and can therefore maintain the original guided mode profile along the TOF propagation similarly with the heating-based fabrication methods.

In this work, we propose and demonstrate a simple and low-cost fabrication method for a TOF-based twisted 2 $\times$ 2 fiber-optic directional coupler using a droplet-based two-step chemical wet-etching process with initial HF acid droplet etching followed by 6:1 buffered HF droplet etching. The droplet-based etching approach takes advantages of the formation of micro-droplets along the optical fibers through the Marangoni effect, and ensures smooth and adiabatic tapering profile [16]. The two-step wet-etching process using both HF and BOE (buffered oxide etch) allows more precise control of the radial etching depth while reducing the roughness of the etched glass surface [17]. The twisted biconical fiber couplers based on the proposed fabrication method show relatively low excess insertion losses ($\sim$0.34 dB), which is comparable to other fabrication techniques [1], [11], [18], [21], [27].

2. Fabrication of TOFs and Twisted Fiber Couplers

2.1 Etch-Based TOF Fabrication and Characterization

Fig. 1(a) shows an overall configuration to fabricate a 2 $\times$ 2 twisted fiber-optic directional coupler using the HF acid-based droplet wet etching technique. Since the optical fiber cladding and core are made of silica materials, they can be easily removed by HF acid-based wet etching. Before making a 2 $\times$ 2 coupler, we first characterized the etch rates of HF and BOE droplets for the silica fibers, and fabricated single-strand TOFs. A bare single mode optical fiber (SMF-28) with an outer radius of 62.5 μm was fixed onto a custom-made acid-resistant styrene cradle, and a 200-μL droplet of 49% HF solution was then placed on a petri dish using a pipette to form a droplet as shown in Fig. 1(b). The volume and size of the acid droplet determines the total etch region (L in Fig. 1(b)),

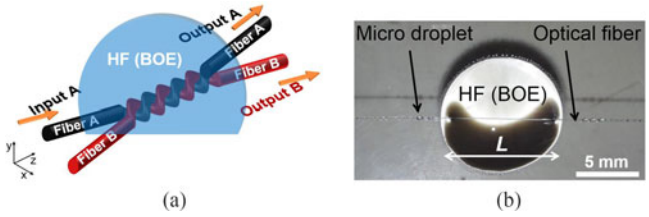

Fig. 1. (a) A schematic drawing and (b) a microscope image of the wet-etching-based fabrication process for a 2 × 2 twisted fiber-optic directional coupler. The immersed length of the optical fiber within the HF acid droplet is L ∼ 9 mm.

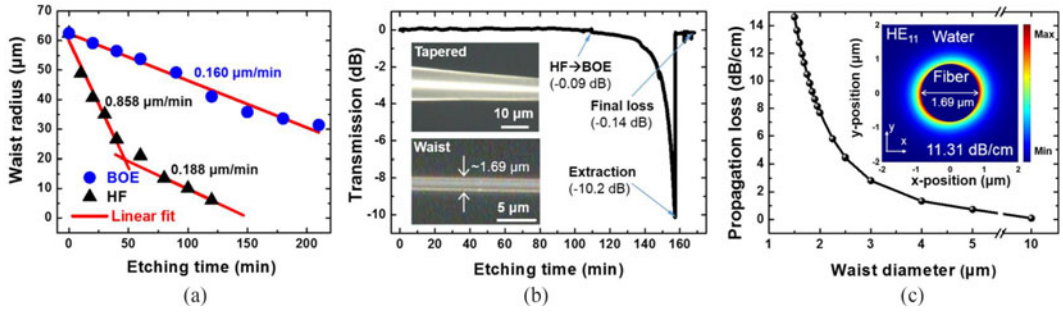

Fig. 2. (a) Etched fiber waist radius as a function of etching time using a 200 μL droplet of HF acid (black triangles) and BOE (blue circles) solution. (b) Optical transmission measurements of a single-strand fiber during the droplet-based chemical etching process. The final optical loss of ∼0.14 dB represents the total insertion loss of the fabricated biconical TOF. The insets represent the optical micrographs of the tapered and waist region of a typical fabricated TOF. (c) Estimated propagation loss as a function of the etched fiber diameter. The inset shows the normalized absorption profile for the fiber diameter of ∼1.69 μm obtained by the FEM simulation. The propagation loss of 11.31 dB/cm was estimated.

and can be changed to obtain different etch length. The overall droplet etching processes were performed at 22 ± 0.5 °C.

As indicated in Fig. 2(a), the radial etch rate for typical optical fibers (SMF-28) using a 200 μL droplet of HF is ∼0.858 μm/min for the first 30 minutes and then gradually decreases. The etch rate of a BOE droplet is much slower and about 0.160 μm/min. The etch rates were obtained by measuring the radii of the etched fibers. Since the silica etch rate depends on the concentrations of HF and HF_2^- in acid solutions, the etch rate using the HF acid droplet decreases with the etching time. However, the etch rate by BOE, which contains both HF and buffer agents, such as ammonium fluoride (NH_4F), remains nearly constant for much longer time (up to ∼100 minutes) as shown in Fig. 2(a). The NH_4F contents of BOE are expected to improve and maintain the etch rate for the extended amount of time because the concentration of more reactive HF_2^- ions increases during the etching process, and the cations NH_4^+ also have catalytic effects on the dissolution reaction of the silica material [28]. As a result, the silica etch rate for a BOE droplet shows a better linearity when compared to that of an HF acid droplet. The slower etch rate of BOE also improves the surface roughness of the tapered region and reduces random surface corrugations to mitigate the optical scattering losses [29]. Furthermore, the final core diameter of the TOF waist region can be more precisely controlled by the constant and more predictable etch rate from a BOE droplet [17].

The measured etch rate from an HF droplet varies significantly over etching time. In the beginning, the HF and BOE etch rates are about 0.858 μm/min and 0.160 μm/min, respectively, which are relatively comparable to the previous reports [17]. However, the overall HF etch rate for longer etching time becomes much slower than the initial rate [17], which may be due to the experimental details such as temperature and humidity [30].

To further verify the two-step etching approach, a single-strand standard single-mode optical fiber (SMF-28) was firstly immersed and etched in an HF acid droplet until the cladding region was mostly removed. When the waist radius of the etched fiber was about 10 μm with the corresponding

HF acid droplet etching time of ∼100 minutes (Fig. 2(a)), the HF droplet was replaced with a 200 μL BOE droplet. In both cases, the length of the optical fiber immersed in the droplet (L in Fig. 1(b)) is approximately 9 mm. During the HF (or BOE) droplet-based chemical etching process, micro-droplets form near the fiber-droplet interface and flow away from the main droplet meniscus region along the fiber by the so-called Marangoni flow [26]. As shown in Fig. 1(b), the concentration of HF in the micro-droplet decreases while it transverses along the fiber, which results in a graded fiber diameter profile and elongated tapered region. The smooth and adiabatic fiber diameter profiles in the TOFs significantly reduce unnecessary optical power coupling between the core and the higher-order cladding modes [31], and eventually provide smaller excess insertion losses preserving the original mode profile.

The fiber diameter and the overall etching progress can be estimated in real-time by monitoring the optical transmission through the etched biconical TOF region at a wavelength of 1.55 μm. Fig. 2(b) represents the measured optical transmission as a function of etching time. When the cladding layer of the optical fiber is not fully etched and therefore the propagating optical mode does not significantly overlap with the surrounding lossy etchant medium, the optical power is not attenuated through the fiber propagation. However, as the cladding layer is further etched away and the fiber core region is exposed to the etchant solution, the propagating optical signal is attenuated along the tapered and waist regions, and the optical power transmission decreases accordingly. When the optical power transmission was about -10 dB, the etched fiber was extracted from the BOE droplet and rinsed by deionized (DI) water to prevent additional chemical etching. The total final insertion loss of ∼0.14 dB was observed after the etched fiber was dried in air. The taper and waist region of a typical fabricated TOF with smooth surface profiles are shown in the insets of Fig. 2(b). Our measurement results (∼10.2 dB loss over $L \sim 9$ mm, or 11.33 dB/cm) agree well with the numerical simulations based on the finite element method (FEM) for the etched fiber diameter of 1.69 μm (Fig. 2(c)). The attenuation constant of the fundamental HE_{11} mode (dominant propagation mode) for the fiber core diameter of ∼1.69 μm with a water cladding layer was calculated to be 11.31 dB/cm (without considering the scattering losses from the surface roughness) due to light absorption into the surrounding water. The propagation loss of the tapered fiber was estimated by obtaining the effective refractive index of the propagation mode with FEM simulations. The complex refractive index of water was assumed to be $1.32 + i1.18 \times 10^{-4}$ [32].

2.2 Fabrication and Characterization of TOF-Based Optical Couplers

To fabricate a TOF-based 2 × 2 twisted fiber-optic directional coupler, we propose simultaneous wet-etching of two twisted optical fibers as schematically described in Fig. 1(a). Two fibers (fiber A and B) are shown in different colors for illustration purposes. The overall device fabrication process is similar to the single-strand TOF fabrication discussed in the previous section. Two single-mode optical fibers (SMF-28) were first twisted with each other for three turns (total rotation angle of 1080°), and then these twisted optical fibers were subsequently immersed together in a 200 μL HF droplet. Before the etching process, the applied optical power at one fiber input was not transferred to the other fiber due to the cladding layer. By simultaneously measuring the optical powers at the output port A (black curve) and B (red curve) in real-time as shown in Fig. 3(a), the optical coupling ratio between the two twisted fibers can be monitored during the droplet-based chemical etching process. The optical power at the input port A (1 mW in our experiments) starts to get gradually transferred to the other fiber (output port B) after about 95 minutes of etching time due to the optical mode overlap between the etched fibers. The optical coupling length continuously decreases because the distance between the two fiber cores decreases with the etching time. We were able to observe the continuous variation of the power splitting ratios with the etching time until the fibers were cut at ∼110 minutes.

As demonstrated by the optical power transfer results shown in Fig. 3(a), the power splitting ratio of the twisted fiber-optic directional coupler can be adjusted by carefully controlling the etching time. To obtain a 50:50 power split ratio in the acid droplet, after approximately 100 minutes, the HF acid droplet was replaced with the low etch rate solution, BOE. The twisted fibers were

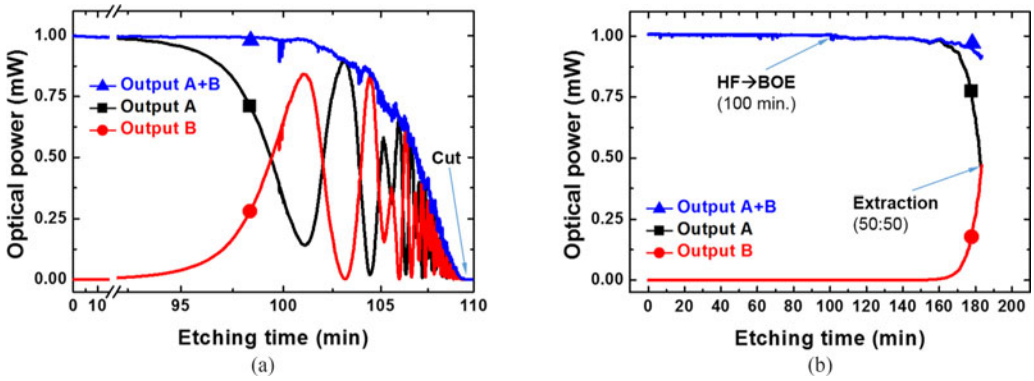

Fig. 3. (a) An example of optical power measurements from the two twisted fibers during the wet-etching process until the fibers are cut. (b) Optical power measurements until the coupling ratio reaches 50:50 in the droplet.

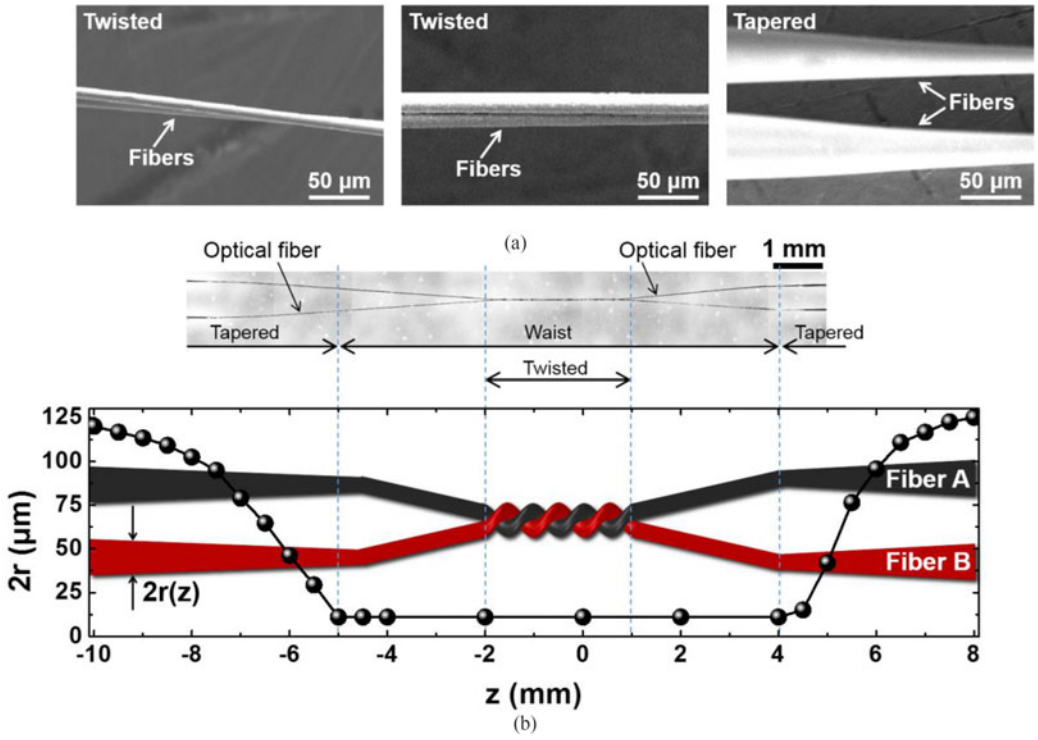

Fig. 4. (a) Typical SEM images of the uniform waist region as well as the smooth tapered surface. (b) An optical micrograph and measured fiber diameter profile for the fabricated coupler. The diameter of the uniform waist region is ∼11 μm. The lengths of the twisted and waist region are ∼3 mm and ∼9 mm, respectively.

extracted from the BOE droplet when the optical powers at the output A and B were almost same (about 0.44 mW at the total etching time of ∼180 minutes as indicated in Fig. 3(b)). The etched fibers were rinsed by DI water to completely remove any remaining acid on the fiber surface, and then dried. The optical coupling ratio was changed to 85:15 after the droplet was dried in air (The optical powers at the output A and B were 0.78 mW and 0.14 mW, respectively.) because of the differences in the refractive index contrast [33]. The optical coupling length between the two TOFs can be modified by the amount of mode overlap, which is influenced by the effective refractive index of the surrounding environments. The excess insertion loss in air was ∼0.34 dB. Fig. 4(a) shows scanning electron microscope (SEM) images of the typical twisted and tapered transition

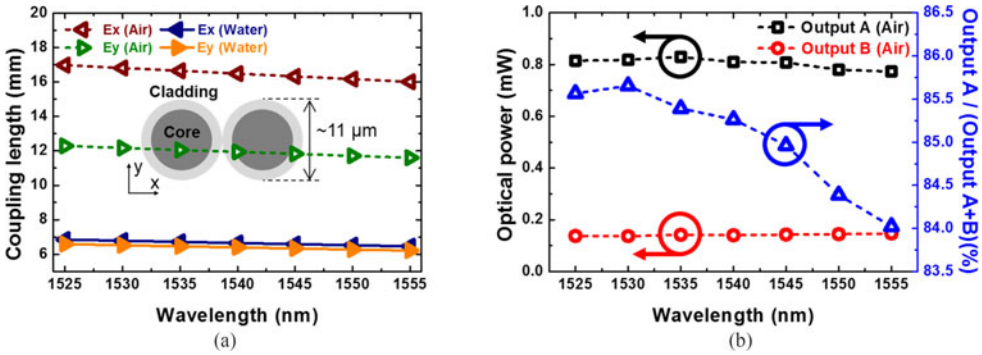

Fig. 5. (a) Coupling lengths of horizontally- (Ex) and vertically-polarized (Ey) inputs according to the different surrounding medium (air: wine and green curves, water: navy and orange curves). The inset shows a schematic cross-section of the two etched fibers. (b) Transmission spectra of the fabricated 2 × 2 coupler. The optical power split ratio varies less than 2% within the telecommunication C-band.

regions. The SEM images also confirm that the two fibers are tightly attached to each other after the wet-etching process because of van der Waals force and capillary attraction. Fig. 4(b) shows an optical micrograph example of a fabricated fiber coupler and the measured fiber diameter profile for the fabricated coupler. We found that the waist region of the biconical TOF had a uniform fiber diameter of ∼11 μm over a total length of ∼9 mm, which roughly corresponds to the fiber length immersed in the droplet (L). The total length of the twisted region is ∼3 mm, and smaller than the droplet size. Because the center of the acid droplet does not exactly coincide with the center of the twisted optical fibers, the diameter profiles exhibit some asymmetry as indicated in Fig. 4(b). However, this asymmetry does not play an important role in the splitting ratio because the whole twisted region remains inside the droplet and the two fibers are sufficiently separated except the twisted region.

To inspect the optical mode guidance for the fabricated fiber-optic coupler with an etched diameter of ∼11.0 μm as depicted in the inset of Fig. 5(a), we numerically calculate the coupling length between the two non-twisted fibers with different surrounding materials (air and water) using the FEM simulations (Fig. 5(a)). According to our simulations, when the fiber diameter is ∼11.0 μm and it is surrounded by water, the optical confinement factor within the fiber region is ∼99.86%. When the etched fiber is surrouned by air, the confinement factor increases to ∼99.96%. Fig. 5(b) shows the measured optical transmission spectra as a function of the input wavelength. We note that the coupling lengths in air for two orthogonal polarizations (E_x and E_y) do not vary significantly over the wide wavelength range covering the whole telecommunication C-band as shown in Fig. 5(a). The variations of the coupling lengths are calculated to be less than 5.6%. The measured transmission spectra over the wavelength range of 1525 ∼ 1555 nm with an input power of 1 mW to the port A is shown in Fig. 5(b). The small power variation over the wide wavelength range agrees qualitatively with the simulated results in Fig. 5(a). As the wavelength increases, the coupling length becomes shorter (stronger interaction between fibers). The measured output power at the output A also gradually decreases with the wavelength as shown in Fig. 5(b). The variation of the power splitting ratio with respect to the input wavelength was about 1.63% within the C-band.

Although rigorous analysis of the twisted coupling region and its birefringence is necessary to fully understand the exact coupling mechanism for the fabricated coupler [34], [35], it is possible to qualitatively estimate its power splitting ratio by simply obtaining the coupling length of the non-twisted coupler with the same fiber diameters. For example, when the etched fibers are in the droplet, the coupling lengths for two orthogonal input polarizations (E_x and E_y) at an input wavelength of 1550 nm are roughly same, and estimated to be ∼6.4 mm according to our simulations (Fig. 5(a)). This indicates that the 50:50 power splitting ratio can be achieved at the etched fiber interacction length of ∼3.2 mm in the droplet (half of the coupling length), which is reasonably consistent with the experimental observation from the fabricated sample shown in Fig. 4(b). The power spitting ratio in air can also be explained in this way. The coupling lengths for two input polarizations are

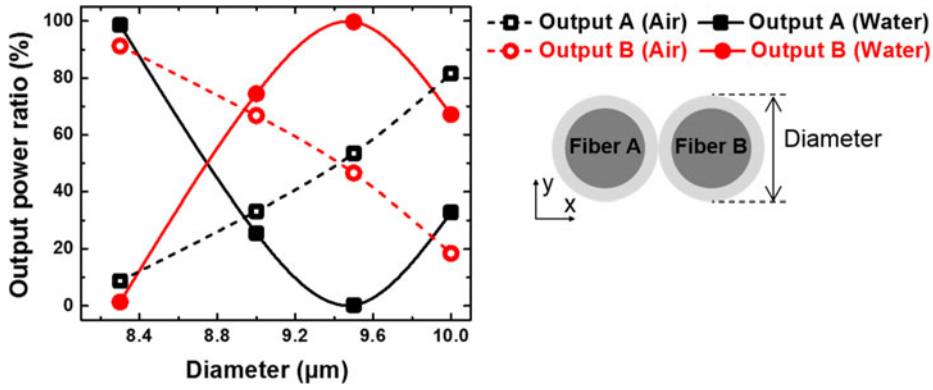

Fig. 6. Estimated output power ratios of two attached micro fibers as a function of the fiber diameters with different surrounding materials. The interaction interval is assumed to be 3.2 mm.

given by $L_{c,x} = 16.2$ mm and $L_{c,y} = 11.7$ mm, respectively. The corresponding coupling constants for two orthogonal polarizations are $C_x = \pi/2L_{c,x} = 0.097\,\text{mm}^{-1}$ and $C_y = \pi/2L_{c,y} = 0.134\,\text{mm}^{-1}$, respectively. Using the optical interaction length of ~3.2 mm, the power splitting ratio for the x-polarized input is given by $\cos^2(C_x \cdot 3.2\text{ mm}) : sin^2(C_x \cdot 3.2\text{ mm}) = 90.7 : 9.3$. For the y-polarized input, it is 82.7:17.3. As described in Fig. 5(b), the actual power splitting ratio is measured to be between these two ratios.

Although the optical power splitting ratio changes with the outer cladding materials (e.g., water or air), it is possible to theoretically predict the power splitting ratios for different cladding materials. As indicated in Fig. 4(b), the overall dimension of the twisted region (main coupling region) can be determined by the droplet size and the number of turns. The optical power splitting ratios with respect to the fiber diameters for different cladding materials can be estimated as exemplified in Fig. 6. For example, to obtain a splitting ratio of ~50:50 in air, the spitting ratio in water needs to be ~1:99 (output A:B).

Finally, since the tapered fiber core is directly exposed, it can be vulnerable to the contamination issues. Such surface contamination problems can be resolved by exposing the micro-fibers to, for example, hexamethyldisilazane after the rinse process as introduced in [16], or applying additional cladding layers to protect the fiber core.

3. Conclusion

In summary, we have demonstrated a simple and cost-effective fabrication scheme for TOF-based twisted 2 × 2 fiber-optic directional couplers using the droplet-based wet-etching process to obtain smooth surface roughness and adiabatic tapering. The proposed fabrication technique with droplet replacement allows fast etching of the fiber cladding region using the higher etch rate of HF as well as a precise and controlled fiber waist region from a lower and consistent etch rate of BOE. Our fabrication results achieve lower excess insertion losses with a relatively short taper length, and the overall excess loss is comparable to other conventional fabrication techniques such as fusion- [11], [18], lapping- [21], [22], and etch-based [1] methods. We believe that the proposed droplet-based fabrication approach can be a promising candidate for simple and low-cost fabrication of various fiber-optic components based on the fiber-optic directional couplers.

References

[1] S. K. Sheem and T. G. Giallorenzi, "Single-mode fiber-optical power divider: Encapsulated etching technique," *Opt. Lett.*, vol. 4, no. 1, pp. 29–31, 1979.

[2] L. Dong, P. Hua, T. Birks, L. Reekie, and P. S. J. Russell, "Novel add/drop filters for wavelength-division-multiplexing optical fiber systems using a Bragg grating assisted mismatched coupler," *IEEE Photon. Technol. Lett.*, vol. 8, no. 12, pp. 1656–1658, Dec. 1996.

[3] S. Korotky *et al.*, "4-Gb/s transmission experiment over 117 km of optical fiber using a Ti: LiNbO 3 external modulator," *J. Lightw. Technol.*, vol. 3, no. 5, pp. 1027–1031, Oct. 1985.
[4] H. Kogelnik and R. V. Schmidt, "Switched directional couplers with alternating $\Delta\beta$," *IEEE J. Quant. Electron.*, vol. 12, no. 7, pp. 396–401, Jul. 1976.
[5] C. Liao, D. Wang, X. He, and M. Yang, "Twisted optical microfibers for refractive index sensing," *IEEE Photon. Technol. Lett.*, vol. 23, no. 13, pp. 848–850, Jul. 2011.
[6] L. Sun *et al.*, "Investigation of humidity and temperature response of a silica Gel coated microfiber coupler," *IEEE Photon. J.*, vol. 8, no. 6, Dec. 2016, Art. no. 6805410.
[7] G. Son, Y. Jung, and K. Yu, "Liquid droplet sensing using twisted optical fiber couplers fabricated by hydrofluoric acid flow etching," *Proc. SPIE*, vol. 10323, 2017, Art. no. 103234J.
[8] K. Li, T. Zhang, G. Liu, N. Zhang, M. Zhang, and L. Wei, "Ultrasensitive optical microfiber coupler based sensors operating near the turning point of effective group index difference," *Appl. Phys. Lett.*, vol. 109, no. 10, 2016, Art. no. 101101.
[9] A. J. Fielding, K. Edinger, and C. C. Davis, "Experimental observation of mode evolution in single-mode tapered optical fibers," *J. Lightw. Technol.*, vol. 17, no. 9, pp. 1649–1656, Sep. 1999.
[10] J.-P. Laine, B. Little, and H. Haus, "Etch-eroded fiber coupler for whispering-gallery-mode excitation in high-Q silica microspheres," *IEEE Photon. Technol. Lett.*, vol. 11, no. 11, pp. 1429–1430, Nov. 1999.
[11] Y. Jung, G. Brambilla, and D. J. Richardson, "Optical microfiber coupler for broadband single-mode operation," *Opt. Exp.*, vol. 17, no. 7, pp. 5273–5278, Mar. 2009.
[12] S. Ko, J. Lee, J. Koo, B. S. Joo, M. Gu, and J. H. Lee, "Chemical wet etching of an optical fiber using a hydrogen fluoride-free solution for a saturable absorber based on the evanescent field interaction," *J. Lightw. Technol.*, vol. 34, no. 16, pp. 3776–3784, Aug. 2016.
[13] J. Wang *et al.*, "Evanescent-light deposition of graphene onto tapered fibers for passive Q-switch and mode-locker," *IEEE Photon. J.*, vol. 4, no. 5, pp. 1295–1305, Oct. 2012.
[14] G. Brambilla, V. Finazzi, and D. Richardson, "Ultra-low-loss optical fiber nanotapers," *Opt. Exp.*, vol. 12, no. 10, pp. 2258–2263, 2004.
[15] L. Ding, C. Belacel, S. Ducci, G. Leo, and I. Favero, "Ultralow loss single-mode silica tapers manufactured by a microheater," *Appl. Opt.*, vol. 49, no. 13, pp. 2441–2445, 2010.
[16] E. J. Zhang, W. D. Sacher, and J. K. Poon, "Hydrofluoric acid flow etching of low-loss subwavelength-diameter biconical fiber tapers," *Opt. Exp.*, vol. 18, no. 21, pp. 22593–22598, 2010.
[17] Z. Chenari, H. Latifi, S. Ghamari, R. Hashemi, and F. Doroodmand, "Adiabatic tapered optical fiber fabrication in two step etching," *Opt. Laser Technol.*, vol. 76, pp. 91–95, 2016.
[18] E. Rawson and M. Bailey, "Bitaper star couplers with up to 100 fibre channels," *Electron. Lett.*, vol. 14, no. 15, pp. 432–433, 1979.
[19] L. Bo, P. Wang, Y. Semenova, and G. Farrell, "Optical microfiber coupler based humidity sensor with a polyethylene oxide coating," *Microw. Opt. Technol. Lett.*, vol. 57, no. 2, pp. 457–460, 2015.
[20] M. Sumetsky, Y. Dulashko, and A. Hale, "Fabrication and study of bent and coiled free silica nanowires: Self-coupling microloop optical interferometer," *Opt. Exp.*, vol. 12, no. 15, pp. 3521–3531, 2004.
[21] M. J. Digonnet and H. J. Shaw, "Analysis of a tunable single mode optical fiber coupler," *IEEE Trans. Microw. Theory Techn.*, vol. 30, no. 4, pp. 592–600, Apr. 1982.
[22] O. Parriaux, S. Gidon, and A. Kuznetsov, "Distributed coupling on polished single-mode optical fibers," *Appl. Opt.*, vol. 20, no. 14, pp. 2420–2423, 1981.
[23] F. Beltrán-Mejía, J. H. Osório, C. R. Biazoli, and C. M. Cordeiro, "D-microfibers," *J. Lightw. Technol*, vol. 31, no. 16, pp. 3056–3061, Aug. 2013.
[24] Y. Zhang, C. Gu, A. Schwartzberg, and J. Zhang, "Surface-enhanced Raman scattering sensor based on D-shaped fiber," *Appl. Phys. Lett.*, vol. 87, no. 12, 2005, Art. no. 123105.
[25] H. S. Haddock, P. Shankar, and R. Mutharasan, "Fabrication of biconical tapered optical fibers using hydrofluoric acid," *Mater. Sci. Eng., B*, vol. 97, no. 1, pp. 87–93, 2003.
[26] R. Tadmor, "Marangoni flow revisited," *J. Colloid Interface Sci.*, vol. 332, no. 2, pp. 451–454, 2009.
[27] Y. Tsujimoto, H. Serizawa, K. Hattori, and M. Fukai, "Fabrication of low-loss 3 dB couplers with multimode optical fibres," *Electron. Lett.*, vol. 5, no. 14, pp. 157–158, 1978.
[28] G. Spierings, "Wet chemical etching of silicate glasses in hydrofluoric acid based solutions," *J. Mater. Sci.*, vol. 28, no. 23, pp. 6261–6273, 1993.
[29] N. Zhong, Q. Liao, X. Zhu, Y. Wang, and R. Chen, "High-quality fiber fabrication in buffered hydrofluoric acid solution with ultrasonic agitation," *Appl. Opt.*, vol. 52, no. 7, pp. 1432–1440, 2013.
[30] A. H. Harvey, J. S. Gallagher, and J. L. Sengers, "Revised formulation for the refractive index of water and steam as a function of wavelength, temperature and density," *J. Phys. Chem. Ref. Data*, vol. 27, no. 4, pp. 761–774, 1998.
[31] A. W. Snyder, "Coupling of modes on a tapered dielectric cylinder," *IEEE Trans. Microw. Theory Techn.*, vol. 18, no. 7, pp. 383–392, Jul. 1970.
[32] W. M. Irvine and J. B. Pollack, "Infrared optical properties of water and ice spheres," *Icarus*, vol. 8, no. 1–3, pp. 324–360, 1968.
[33] M. Centeno, "The refractive index of liquid water in the near infra-red spectrum," *J. Opt. Soc. Amer.*, vol. 31, no. 3, pp. 244–247, 1941.
[34] T. Birks, "Twist-induced tuning in tapered fiber couplers," *Appl. Opt.*, vol. 28, no. 19, pp. 4226–4233, 1989.
[35] K. Morishita and T. Yamaguchi, "Wavelength tunability and polarization characteristics of twisted polarization beam-splitting single-mode fiber couplers," *J. Lightw. Technol.*, vol. 19, no. 5, pp. 732–738, May 2001.